Journal of Network Intelligence
Taiwan Ubiquitous Information
 ISSN 2414-8105 (Online)
Volume **7**, Number **1**, February **2022**

Multi-histogram Reversible Data Hiding with Contrast Enhancement

Shaowei Weng[1], Ye, Zhou[2], Bingbing You[1], Tiancong Zhang[1]*
Caijie, Yang[1], Chunyu Zhang[3], Yunqing Shi[4]

[1]School of Electronic, Electrical Engineering and Physics
Fujian University of Technology
Fuzhou, 350118, China
wswweiwei@126.com, kushentian@163.com, 1040945310@qq.com, 1010629433@qq.com

[2]School of Computer Science and Mathematics
Fujian University of Technology
Fuzhou, 350118, China
1962270759@qq.com

[3]College of information engineering
Xizang Minzu university, Xianyang 712082, China
zcy@xzmu.edu.cn

[4]Department of Electrical and Computer Engineering
New Jersey Institute of Technology, Newark, NJ 07103 USA
shi@njit.edu

Received November 2021; revised January 2022
(*Corresponding Author: kushentian@163.com)

Abstract. *The basic principle of reversible data hiding with contrast enhancement abbreviated as RDH-CE is to enhance the perceived contrast of stego images using an reversible data-embedding manner. Considering that existing RDH-CE methods can only enhance the global contrast of the image but ignore or may even reduce the local contrast, an RDH-CE method combining K-means clustering with multiple features is proposed in this paper. K-means clustering with multiple features is employed to yield multiple histograms. Adaptive contrast enhancement based on the local properties of multiple histograms is applied to enhance the local contrast as well as global contrast while achieving satisfactory embedding capacity. The experimental results also demonstrate the effectiveness of the proposed method.*
Keywords: Reversible data hiding, Contrast enhancement, Genetic algorithm, Multiple histogram

1. **Introduction.** Differently from digital watermarking [1, 2] that aims at increasing robustness against attacks, data hiding focuses on achieving high capacity imperceptibly. Reversible data hiding (RDH), as a special branch of data hiding, has the capabilities of exactly recovering the stego image to its original state after extracting the embedded data. Depending on its capabilities, RDH are useful at some applications such as military imaging, medical imaging or law enforcement, where permanent distortion is not allowed. Up to now, RDH has been extensively investigated and a large number of RDH methods have been proposed from the following perspectives: lossless compression [3, 4], difference expansion (DE) [5], histogram shifting (HS) [6], prediction error expansion (PEE) [7–10], integer-to-integer transform [4, 11–14]. Among the aforementioned techniques, DE is a classical work of RDH, which was firstly proposed by Tian [5] to embed one bit into

the least significant bit of the expanded difference. Another classical work of RDH is HS that was proposed by Ni *et al.* [6] to select peak bins of the image histogram for embedding data while shifting other bins for guaranteing reversibility. HS produces a high quality stego image but the embedding capacity is limited by the peak height of the image histogram. Thodi *et al.* [7] proposed PEE (an improved version of DE) by expanding prediction errors, rather than difference values in DE for embedding data. Subsequently, some methods extended the PEE by improving the performance of the predictor, such as gradient-adjusted predictor [15], rhombus predictor [16], and pixel-value-ordering [17–19], to generate a prediction-error histogram (PEH) with a sharper distribution. To maintain high visual quality, HS is introduced into these methods to modify the PEH for embedding data. We term the methods of this type combining HS and PEE as PEE-HS based methods. PEE-HS based methods have gradually become one of the mainstream methods for RDH owing to their efficient capacity-distortion tradeoff. However, traditional PEE-HS based methods uniformly modify the entire PEH without consideration of the local properties of prediction errors. To this end, Li *et al.* [20] proposed a multiple histograms modification (MHM) based RDH method by adaptively selecting embedding bins for each histogram. In their method, the entire PEH is split into 16 equal-sized histograms according to the local complexities of prediction errors. The rate-distortion is formulated and solved using exhaustive search, so that the embedding bins for multiple histograms achieving the highest PSNR at a given payload are obtained. Inspired by Li *et al.*'s method, Wang *et al.* [21] proposed to utilize fussy C-means equipped with multiple features to obtain multiple sharply distributed histograms. Weng *et al.* [22] proposed to establish multiple histograms by exploiting K-means clustering with multiple-features and utilize the improved crisscross optimization algorithm with a fast convergence speed to search optimal embedding bins for each histogram. Wang *et al.* proposed an RDH general framework with MHM, in which multiple histograms are constructed based on optimized multi-features, and the rate allocation is formulated and solved with genetic algorithm [23].

In a word, the RDH methods proposed so far focus on largely increasing the embedding capacity without degrading the image quality. In RDH methods, the peak signal-to-noise ratio (PSNR) is most frequently used for evaluating the visual quality. However, these methods seldom consider increasing the perceived contrast of the stego image. For example, for poorly illuminated images, increasing the visual image quality such as image contrast is more important than simply keeping high PSNR values. Histogram equalization [24] is one of the most popularly used methods for contrast enhancement. Wu *et al.* [25] proposed an RDH method with contrast enhancement (RDH-CE) that aims at enhancing the image contrast as well as providing a high embedding capacity. Effectively, the image contrast enhancement can be achieved by spreading the limited dramatic distributed histogram as evenly and broadly as possible to the whole grayscale range $[0, 255]$. Specifically, their method spread pixel values towards two ends of the whole grayscale range by recursively performing HS, so that the image contrast is enhanced and high embedding capacity is achieved. Several methods have been proposed to achieve more contrast enhancement effects and higher embedding capacity [26–32]. Besides, some researchers have extended RDH-CE to medical images [29, 33]. Among the aforementioned techniques, Jafar *et al.* [27] proposed to split the image into five categories using K-means clustering, and adaptively perform the local contrast enhancement as well as increase the embedding capacity according to the local property of each category. Kim *et al.* [31] proposed to enhance the contrast using an adaptive bin selection process based on brightness preservation [31].

After carrying out several observations on Jafar *et al.* [27], it is found that Jafar *et al.*'s method provides no payload but merely causes undesirable image distortion because the global contrast of the image is enhanced by stretching the global histogram without considering embedding data. The second observation is that K-means clustering equipped with a single feature does not exactly evaluate the local complexity of each pixel to be predicted, and therefore cannot generate five more sharply-distributed categories. Finally, Jafar *et al.*'s method cannot differently treat Types II to IV, and thus, cannot perform the local contrast enhancement in an adaptive manner for Types II to IV.

In this paper, we propose a novel RDH-CE method based on K-means clustering with multiple subtly designed features. K-means clustering with multiple subtly-designed features are utilized to generate multiple sharply-distributed categories. The spreading range is allocated for each category, and then, the global contrast enhancement is achieved by spreading each category using HS across the allocated grayscale range. Each category is processed adaptively according to the local property of each histogram. The pixels are processed locally based on the local complexity.

The rest of this paper is organized as follows. The proposed method is presented in Section 2. The experimental result is discussed in Section 3 while the conclusion is given in Section 4.

2. **The proposed method.**

In this section, several parts of the proposed method will be introduced one by one.

2.1. **Global contrast.**

According to the aforementioned description, Jafar *et al.*'s method utilizes histogram stretching to achieve the global contrast, which makes no contribution to increase the payload. Differently from Jafar *et al.*'s method, the genetic algorithm (GA) is firstly used in the proposed method to select multiple bins for the global contrast as well as data embedding. In this paper, the maximum and minimum pixel values of a cover image with size $M \times N$ are denoted by $\mathcal{L}_G$ and $\mathcal{S}_G$, respectively. Taking Lena for example, $\mathcal{S}_G = 26$ and $\mathcal{L}_G = 245$. GA is utilized to select multiple optimal bins from both sides of the image histogram which achieve the highest rate-distortion performance, and subsequently, HS is repeatedly performed to achieve both data embedding and contrast enhancement. From Fig. 1, it is obvious that GA is used to search 26 optimal bits on the left side of the image histogram and 10 optimal bins on the right side of the histogram.

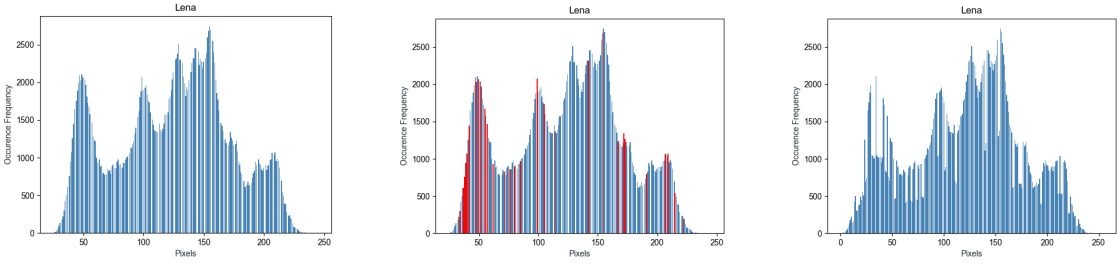

(a) (b) (c)

FIGURE 1. A simple example. (a) Original image histogram, (b) Original image histogram that uses GA to select multiple bins marked in red. (c) The image with the global contrast enhancement and the payload of $43,097$ bits.

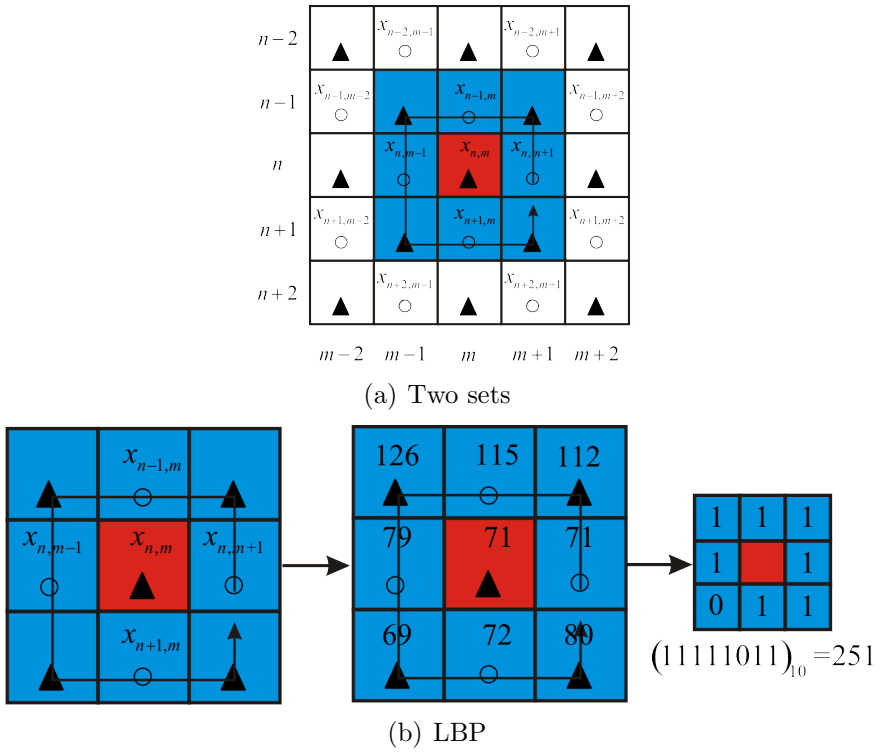

(a) Two sets

(b) LBP

FIGURE 2. Two sets S_α marked in "▲" and S_β marked in "○".

2.2. **Multiple histograms.** All the pixels are split into two disjoint sets: S_α and S_β in the same way as the layout of a chessboard, which are marked by "▲" and "○", respectively, as shown in Fig. 2. Two sets are processed in the same manner. Here, we only discuss the set S_α. Specifically, each pixel in S_α is predicted by its nearest pixels from S_β. Simultaneously, multiple features of each pixel in S_α extracted from the local complexities are determined by the pixels in S_β. During data embedding, all the pixels in S_β must remain unaltered. Before prediction, multiple features need to be extracted, so that five histograms are constructed using K-means with multiple features. Here, multiple features are described one by one.

(1) Sobel masks. For a pixel $x_{n,m}$ in S_α, Sobel masks [34, 35] is calculated as

$$f^1_{m,n} = \sqrt{\nabla_h^2 + \nabla_v^2}, \tag{1}$$

where $\nabla_h = \sum_{k=-1}^{1} r_k \left[x_{n+k,m+1} - x_{n+k,m-1}\right]$ and $\nabla_v = \sum_{k=-1}^{1} r_k \left[x_{n+1,m+k} - x_{n-1,m+k}\right]$. $r_k = 2$ for $k = 0$ while $r_k = 1$ for $k \neq 0$. Referring to Eq. (1), the four neighbors of $x_{m,n}$, i.e., $x_{n-1,m-1}$, $x_{n-1,m+1}$, $x_{n+1,m-1}$ and $x_{n+1,m-1}$, involve calculating $\nabla_{(h,v)}$. However, those neighbors may be changed during data embedding because they belong to the same set S_α as $x_{m,n}$. To guarantee reversibility and simultaneously apply Sobel masks to the pixels in S_α, Eq. (2) is used to generate all eight neighbors of $x_{n,m}$ using the pixels in S_β. As formulated in Eq. (2), each of $x_{n-1,m-1}$, $x_{n-1,m+1}$, $x_{n+1,m-1}$ and $x_{n+1,m-1}$ is replaced by the mean value of its top, bottom, left and right neighbors.

$$x_{n,m} = \begin{cases} x_{n,m}, & \text{if } x_{n,m} \in S_\alpha; \\ \mu, & \text{otherwise.} \end{cases} \tag{2}$$

where $\mu = (x_{n+1,m}+x_{n-1,m}+x_{n,m+1}+x_{n,m-1})/4$.

(2) The intensity variations of pixels in four directions, namely horizonal ($\sigma^2_{t_0}$), vertical ($\sigma^2_{t_{90}}$), 45^o ($\sigma^2_{t_{45}}$) diagonal and 135^o diagonal ($\sigma^2_{t_{135}}$) directions. The efficient adaptive prediction (EAP) predictor [36] is described as follows. In EAP, the eight neighbors of $x_{n,m}$ are split into four sets, namely t_0, t_{45}, t_{90} and t_{135}, where $t_0 = \{x_{n,m-1}, x_{n,m+1}, \mu_0\}$, $t_{45} = \{x_{n,m+1}, x_{n+1,m}, \mu_{45}\}$, $t_{90} = \{x_{n+1,m}, x_{n-1,m}, \mu_{90}\}$, $t_{135} = \{x_{n,m-1}, x_{n+1,m}, \mu_{135}\}$. Here, $\mu_0 = (x_{n,m-1}+x_{n,m+1})/2$, $\mu_{45} = (x_{n,m+1}+x_{n+1,m})/2$, $\mu_{90} = (x_{n+1,m}+x_{n-1,m})/2$ and $\mu_{135} = (x_{n,m-1}+x_{n+1,m})/2$.

Four parameters are applied to measure intensity variation of pixels in four directions, namely horizonal ($\sigma^2_{t_0}$), vertical ($\sigma^2_{t_{90}}$), 45^o ($\sigma^2_{t_{45}}$) diagonal and 135^o diagonal ($\sigma^2_{t_{135}}$) directions.

$$\begin{cases} \sigma^2_{t_0} &= \sum_{k=1}^{3} (t_0(k) - \mu)^2; \\ \sigma^2_{t_{45}} &= \sum_{k=1}^{3} (t_{45}(k) - \mu)^2; \\ \sigma^2_{t_{90}} &= \sum_{k=1}^{3} (t_{90}(k) - \mu)^2; \\ \sigma^2_{t_{135}} &= \sum_{k=1}^{3} (t_{135}(k) - \mu)^2; \end{cases} \tag{3}$$

where $\mu = (\mu_0 + \mu_{45} + \mu_{90} + \mu_{135})/4$. Therefore, $f^2_{n,m} = \sqrt{(\sigma^2_{t_0} + \sigma^2_{t_{45}} + \sigma^2_{t_{90}} + \sigma^2_{t_{135}})}$.

(3) Mean value of V containing four neighbors surrounding $x_{n,m}$, namely $f^3_{n,m} = \mu$, where $V = \{x_{n,m-1}, x_{n,m+1}, x_{n-1,m}, x_{n+1,m}\}$.

(4) Maximum pixel of V, namely $f^4_{n,m} = \max\{V\}$.

(5) Minimum pixel of V, namely $f^5_{n,m} = \min\{V\}$.

(6) The 6^{th} feature $f^6_{n,m}$, namely the local variance of V, is calculated as following:

$$f^6_{n,m} = \sum_{x \in V} (x - \mu)^2. \tag{4}$$

(7) Local variance of four horizonal pixels centered at $x_{n,m}$ is calculated below:

$$f^7_{n,m} = \sum_{k=m-3,m-1,m+1,m+3} (x_{n,k} - \mu_h), \tag{5}$$

where μ_h is the mean value of $x_{n,m-3}$, $x_{n,m-1}$, $x_{n,m+1}$ and $x_{n,m+3}$.

(8) Local variance of four vertical pixels centered at $x_{n,m}$ is obtained using the rule:

$$f^8_{n,m} = \sum_{k=n-3,n-1,n+1,n+3} (x_{k,m} - \mu_v), \tag{6}$$

where μ_v is the mean value of $x_{n-3,m}$, $x_{n-1,m}$, $x_{n+1,m}$ and $x_{n+3,m}$.

(9) As illustrated in Fig. 2, $f^9_{n,m}$ also applied in [22] indicates the sum of the horizontal and vertical differences of a 5×5-sized block centered at $x_{n,m}$.

$$f^9_{n,m} = \sum_{a=1}^{7} \left(|s_u[a] - s_b[a]| + |s_l[a] - s_r[a]| \right), \tag{7}$$

where the symbols $s_u = \{x_{n-1,m-2}, x_{n-2,m-1}, x_{n,m-1}, x_{n-1,m}, x_{n-2,m+1}, x_{n,m+1}, x_{n-1,m+2}\}$, $s_b = \{x_{n+1,m-2}, x_{n,m-1}, x_{n+2,m-1}, x_{n+1,m}, x_{n,m+1}, x_{n+2,m+1}, x_{n+1,m+2}\}$, $s_l = \{x_{n-2,m-1}, x_{n-1,m-2}, x_{n-1,m}, x_{n,m-1}, x_{n+1,m-2}, x_{n+1,m}, x_{n+2,m-1}\}$, $s_r = \{x_{n-2,m+1}, x_{n-1,m}, x_{n-1,m+2}, x_{n,m+1}, x_{n+1,m}, x_{n+1,m+2}, x_{n+2,m+1}\}$, and $[a]$ represents the a^{th} pixel of a set.

(10) Referring to Fig. 2, $f^{10}_{n,m}$ also used in [22] indicates the local invariance of pixels marked in "▲".

$$f^{10}_{n,m} = \sum_{x \in S_\alpha} (|x - \bar{\mu}|), \tag{8}$$

where $\bar{\mu}$ is the average value of pixels marked in "○" of a 5×5-sized block shown in Fig. 2.

2.3. **Local contrast.** K-means clustering with multiple features are used for generating five histograms, and then sorted according to the ascending order of the entropies of histograms to generate five sorted histograms, namely h_1 (smooth), h_2 (near smooth), h_3 (weak edge), h_4 (moderate edge) and h_5 (strong edge). Specifically, the entropy of the κ^{th} histogram is calculated by

$$E_l = \sum_{k\in[0,255]} -p_k \log p_k, \tag{9}$$

where p_k denotes the occurrence frequency of the pixels valued k in each histogram. The pixels belonging to different histograms are processed differently to achieve data embedding and contrast enhancement, and simultaneously alleviate the problems of local contrast enhancement.

As we know, introducing small changes to the pixels in h_1 for enhancing the contrast inevitably degrades the visual quality like noise amplification. Stretching the pixels in h_5 that contains strong edges will result in excessive edge enhancement. To alliterate the problems associated with noise amplification in smooth regions and excessive enhancement of strong edges, each pixel in $h_1 \cup h_5$ is slightly modified using HS via Eq. (10) for data embedding without consideration of contrast enhancement.

$$x^{'} = \begin{cases} x - b, & \text{if } x = x_{lp}; \\ x + b, & \text{if } x = x_{rp}; \\ x, & \text{if } x \in (x_{rp}, x_{lp}); \\ x + 1, & \text{if } x > x_{rp}; \\ x - 1, & \text{if } x < x_{lp}; \end{cases} \tag{10}$$

where x_{lp} and x_{rp} represent left and right peak points of the histogram, respectively, b is a bit to be embedded, namely $b \in \{0, 1\}$. The reverse process of Eq. (10) is given by

$$x = \begin{cases} x^{'}, & \text{if } x^{'} \in [x_{rp}, x_{lp}]; \\ x^{'} - 1, & \text{if } x^{'} \geq x_{rp} + 1; \\ x^{'} + 1, & \text{if } x^{'} \leq x_{lp} - 1. \end{cases} \tag{11}$$

2.3.1. *Modifying h_2 to h_4.* For the current pixel $x_{n,m}$ of the κ^{th} h_κ, it is predicted by its top, bottom, left and right neighbors to generate the prediction value $x^{'}_{n,m}$, namely $x^{'}_{n,m} = \mu$. Each prediction error $e_{n,m}$ is calculated to be $e_{n,m} = x_{n,m} - x^{'}_{n,m}$, so that the prediction error histogram (PEH) HP_κ is generated.

As an evolutionary optimization algorithm, the genetic algorithm (GA) is firstly used in this paper to automatically search for multiple optimal bins for different PEHs while achieving contrast enhancement and data embedding. As we know, GA has the capability of powerful global search and fast convergence speed, which can guarantee efficient search in the huge solution space.

Before utilizing GA to search for multiple optimal bins for each PEH of HP_2 to HP_4, we need to allocate the desired capacity $\mathcal{P}$ to three histograms (HP_2 to HP_4), namely $\mathcal{P}_2$ to $\mathcal{P}_4$. For simplification, $\mathcal{P}_3 = \mathcal{P}_2 + \mathcal{P}_4$ and $\mathcal{P}_2 = \mathcal{P}_4$. After performing the capacity allocation, GA is utilized to select multiple optimal bins from both sides of each PEH which achieve the highest rate-distortion performance under the allocated capacity, and subsequently, HS is repeatedly performed to embed $\mathcal{P}_l$ into the prediction errors of the κ^{th} h_κ while achieving contrast enhancement. Let the selected bins of HE be $p_{\kappa,l_\omega} < \cdots < p_{\kappa,l_2} < p_{\kappa,l_1} < 0 \leq p_{\kappa,r_1} < p_{\kappa,r_2} < \cdots < p_{\kappa,r_\upsilon}$. During data embedding, each prediction

error is modified below

$$e^{'} = \begin{cases} e, & \text{if } p_{\kappa,l_1} < e < p_{\kappa,r_1}; \\ e-(i-1)-b, & \text{if } e = p_{\kappa,l_i}; \\ e+(j-1)+b, & \text{if } e = p_{\kappa,r_j}; \\ e-i, & \text{if } p_{\kappa,l_{i+1}} < e < p_{\kappa,l_i}; \\ e+j, & \text{if } p_{\kappa,r_j} < e < p_{\kappa,r_{j+1}}; \end{cases} \tag{12}$$

where $i \in \{1, 2, \cdots, \omega\}$ and $j \in \{1, 2, \cdots, \upsilon\}$. The reverse operation of Eq. (13) is expressed by

$$e = \begin{cases} e^{'}, & \text{if } p_{\kappa,l_1} < e^{'} < p_{\kappa,r_1}; \\ e^{'}+(i-1), & \text{if } e^{'} = p_{\kappa,l_i}; \\ e-(j-1), & \text{if } e^{'} = p_{\kappa,r_j}; \\ e+i, & \text{if } p_{\kappa,l_{i+1}} < e^{'} < p_{\kappa,l_i}; \\ e-j, & \text{if } p_{\kappa,r_j} < e^{'} < p_{\kappa,r_{j+1}}; \end{cases} \tag{13}$$

3. **Experimental results.** Several experiments are carried out to demonstrate the effectiveness of the proposed method. As shown in Fig. 1, four classical images including Lena, Baboon, Peppers, Airplane and Barbara taken from USC-SIPI [37] are used as test images.

(a) Lena (b) Baboon (c) Peppers (d) Airplane (e) Barbara

FIGURE 3. five test images.

To validate the capability of the proposed method in enhancing the contrast and strengthening the edges in the image, the well-known image sharpness measure Tenegrad (TEN) [38] is employed in the proposed method to measure the contrast enhancement.

$$TEN = \sum_n \sum_m f^1_{m,n} \ , \ \text{if } f^1_{m,n} > \mu_t; \tag{14}$$

where $f^1_{n,m}$ is the Sobel gradient magnitude value [34, 35] computed in Eq. (1) and μ_t is a predefined threshold value that is chosen in the experiments as the mean value of all Sobel gradient magnitude values.

The non-reference metric Q [39] is given by

$$Q = \sum\nolimits_{k=1}^{N} Q_k \Big/ N, \tag{15}$$

where $Q_k = s_1 \times (s_1 - s_2)/(s_1 + s_2)$, and $s_1, s_2, \cdots$, are the singular values satisfying $s_1 \geqslant s_2 \geqslant \cdots \geqslant 0$. $N = \lfloor (H \times W)/(8 \times 8) \rfloor$ denotes the number of disjoint image blocks of size 8×8 for a $H \times W$-sized image. A larger Q implies the better contrast of the stego image.

Five figures including Fig. 4 to Fig. 8 reveal visually that the proposed method has the capability of enhancing the image contrast. In addition, these figures clearly show the proposed method achieves larger Q and TEN.

(a) (b)

FIGURE 4. Lena and the corresponding stego image with $PSNR = 31.78$ dB under a capacity of $161,061$ bits. (a) Original Lena with $TEN = 9.0295$ and $Q = 74.2732$; (b) The stego image for Lena with $TEN = 10.1530$ and $Q = 81.9170$.

(a) (b)

FIGURE 5. Airplane and the corresponding stego image with $PSNR = 28.33$ dB under a capacity of $176,854$ bits. (a) Original Airplane with $TEN = 10.9043$ and $Q = 83.5543$; (b) The stego image for Airplane with $TEN = 12.1593$ and $Q = 95.7003$.

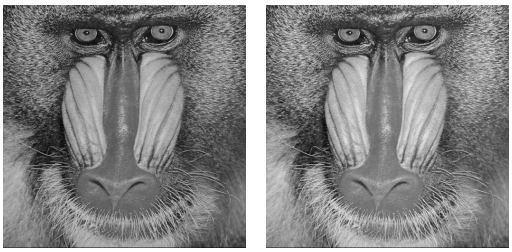

(a) (b)

FIGURE 6. Baboon and the corresponding stego image with $PSNR = 36.38$ dB under a capacity of $61,763$ bits. (a) Original Baboon with $TEN = 21.7174$ and $\bar{C} = 190.3886$; (b) The stego image for Baboon with $TEN = 21.8939$ and $\bar{C} = 191.7313$.

4. **Conclusions.** In this paper, we proposed a multi-histogram reversible data hiding method with contrast enhancement. Multiple histograms are processed differently with the consideration of the local properties of histograms. Considering that stretching excessively the pixels in h_1 and h_5 for improving the contrast inevitably causes the problems associated with noise amplification or over enhancement, the pixels in h_1 and h_5 are modified using HS to carry data so that satisfactory visual quality can be maintained. h_2 to h_4 are adaptively modified to achieve the local and global contrast while embedding the required capacity. GA is used in h_2 to h_4 to adaptively select multiple optimal embedding

(a) (b)

FIGURE 7. Peppers and the corresponding stego image with $PSNR = 33.39$ dB under a capacity of $100,919$ bits. (a) Original Peppers with $TEN = 8.2019$ and $Q = 81.4708$; (b) The stego image for Peppers with $TEN = 8.4910$ and $Q = 82.7411$.

(a) (b)

FIGURE 8. Barbara and the corresponding stego image with $PSNR = 38.24$ dB under a capacity of $83,841$ bits. (a) Original Barbara with $TEN = 15.0979$ and $Q = 129.0935$; (b) The stego image for Barbara with $TEN = 15.2138$ and $Q = 131.3552$.

bins for each histogram. Experimental results revealed the effectiveness of the proposed method in terms of the embedding capacity and contrast enhancement.

Acknowledgments. This work was supported in part by the National NSF of China under Grant 61872095, Grant 61571139, Grant 61872128, in part International Scientific and Technological Cooperation of Guangdong Province under Grant 2019A050513012, in part by the Open Project Program of Shenzhen Key Laboratory of Media Security under Grant ML-2018-03, in part by Fujian Science Fund for Distinguished Young Scholars under Grant 2020J06043.

REFERENCES

[1] H.-C. Huang, S.-C. Chu, J.-S. Pan, C.-Y. Huang, and B.-Y. Liao, "Tabu search based multi-watermarks embedding algorithm with multiple description coding," *Information Sciences*, vol. 181, no. 16, pp. 3379–3396, 2011.

[2] J.-S. Pan, X.-X. Sun, S.-C. Chu, A. Abraham, and B. Yan, "Digital watermarking with improved SMS applied for QR code," *Engineering Applications of Artificial Intelligence*, vol. 97, 2021, doi.org/10.1016/j.engappai.2020.104049.

[3] G. R. Xuan, C. Y. Yang, Y. Z. Zhen, and Y. Q. Shi, "Reversible data hiding using integer wavelet transform and companding technique," in *Proceedings of International Workshop on Digital-forensics and Watermarking*, vol. 5, 2004, pp. 23–26.

[4] X. Wang, X. L. Li, B. Yang, and Z. M. Guo, "Efficient generalized integer transform for reversible watermarking," *IEEE signal processing letters*, vol. 17, no. 6, pp. 567–570, 2010.

[5] J. Tian, "Reversible data embedding using a difference expansion," *Digital Signal Processing*, vol. 13, no. 8, pp. 890–896, 2003.
[6] Z. Ni, Y. Q. Shi, N. Ansari, and W. Su, "Reversible data hiding," *Digital Signal Processing*, vol. 16, pp. 354–362, 2006.
[7] M. Thodi and J. J. Rodríguez, "Prediction-error based reversible watermarking," in *Proceedings of IEEE International Conference on Image Processing*, vol. 3, 2004, pp. 1549–1552.
[8] S. W. Weng, J.-S. Pan, and L. D. Li, "Reversible data hiding based on an adaptive pixel-embedding strategy and two-layer embedding," *Information Sciences*, vol. 369, pp. 144–159, 2016.
[9] S. W. Weng, Y. Q. Shi, W. Hong, and Y. Yao, "Dynamic improved pixel ordering reversible data hiding," *Information Sciences*, vol. 489, pp. 136–154, 2019.
[10] R. Geetha and S. Geetha, "Multi-layered "plus-minus one" reversible data embedding scheme," *Journal of Information Hiding and Multimedia Signal Processing*, vol. 11, no. 2, pp. 58–69, 2020.
[11] A. M. Alattar, "Reversible watermark using the difference expansion of a generalized integer transform," *IEEE Transactions on Image Processing*, vol. 13, no. 8, pp. 1147–1156, 2004.
[12] X. Wang, X. L. Li, and B. Yang, "High capacity reversible image watermarking based on integer transform," in *Proceedings of IEEE International Conference on Image Processing*, 2010, pp. 217–220.
[13] F. Peng, X. Li, and B. Yang, "Adaptive reversible data hiding scheme based on integer transform," *Signal Processing*, vol. 92, no. 1, pp. 54–62, 2012.
[14] S. W. Weng, S.-C. Chu, N. Cai, and R. Zhan, "Invariability of mean value based reversible watermarking," *Journal of Information Hiding and Multimedia Signal Processing*, vol. 4, no. 2, pp. 90–98, 2013.
[15] M. Fallahpour, "Reversible image data hiding based on gradient adjusted prediction," *IEICE Electron Express*, vol. 5, no. 20, pp. 870–876, 2008.
[16] V. Sachnev, H. J. Kim, J. Nam, S. Suresh, and Y. Q. Shi, "Reversible watermarking algorithm using sorting and prediction," *Digital Signal Processing*, vol. 19, no. 7, pp. 989–999, 2009.
[17] X. L. Li, J. Li, B. Li, and B. Yang, "High-fidelity reversible data hiding scheme based on pixel-value-ordering and prediction-error expansion," *Signal Processing*, vol. 93, no. 1, pp. 198–205, 2013.
[18] F. Peng, X. L. Li, and B. Yang, "Improved pvo-based reversible data hiding," *Digital Signal Processing*, vol. 25, pp. 255–265, 2014.
[19] B. Ou, X. L. Li, and J. W. Wang, "Improved PVO-based reversible data hiding: A new implementation based on multiple histograms modification," *Journal of Visual Communication and Image Representation*, vol. 22, no. 12, pp. 5010–5021, 2014.
[20] X. L. Li, W. M. Zhang, X. L. Gui, and B. Yang, "Efficient reversible data hiding based on multiple histograms modification," *IEEE Transactions on Information Forensics and Security*, vol. 10, no. 9, pp. 2016–2027, 2015.
[21] J. X. Wang, N. X. Mao, X. Chen, J. Q. Ni, and Y. Q. Shi, "Multiple histograms based reversible data hiding by using fcm clustering," *Signal Processing*, vol. 159, pp. 193–203, 2019.
[22] S. W. Weng, W. L. Tan, B. Ou, and J.-S. Pan, "Reversible data hiding method for multi-histogram point selection based on improved crisscross optimization algorithm," *Information Sciences*, vol. 549, pp. 13–33, 2021.
[23] J. X. Wang and X. Chen and J. Q. Ni and N. X. Mao and Y. Q. Shi, "Multiple histograms-based reversible data hiding: framework and realization," *IEEE Transactions on Circuits and Systems for Video Technology*, vol. 30, no. 8, pp. 2313–2328, 2020.
[24] J. A. Stark, "Adaptive image contrast enhancement using generalizations of histogram equalization," *IEEE Transactions on Image Processing*, vol. 9, no. 5, pp. 889–896, 2000.
[25] H. T. Wu, J.-L.Dugelay, and Y.-Q. Shi, "Reversible image data hiding with contrast enhancement," *IEEE signal processing letters*, vol. 22, no. 1, pp. 81–85, 2015.
[26] G. Y. Gao and Y.-Q. Shi, "Reversible data hiding using controlled contrast enhancement and integer wavelet transform," *IEEE signal processing letters*, vol. 22, no. 11, pp. 2078–2082, 2015.
[27] I. F. Jafar, K. A. Darabkh, and R. R. Saifan, "SARDH: A novel sharpening-aware reversible data hiding algorithm," *Journal of Visual Communication and Image Representation*, vol. 39, no. 8, pp. 239–252, 2016.
[28] H. S. Chen, J. Q. Ni, W. Hong, and T.-S. Chen, "Reversible data hiding with contrast enhancement using adaptive histogram shifting and pixel value ordering," *Signal Processing: Image Communication*, vol. 16, pp. 1–16, 2016.

[29] G. Y. Gao, X. D. Wan, S. M. Yao, Z. M. Cui, C. X. Zhou, and X. M. Sun, "Reversible data hiding with contrast enhancement and tamper localization for medical images," *Information Sciences*, vol. 385-386, pp. 250–265, 2017.
[30] H. T. Wu, S. H. Tang, J. W. Huang, and Y. Q. Shi, "A novel reversible data hiding method with image contrast enhancement," *Signal Processing: Image Communication*, vol. 62, pp. 64–73, 2018.
[31] S. Kim, R. L. X. C. Qu, F. J. Huang, and H. J. Kim, "Reversible data hiding with automatic brightness preserving contrast enhancement," *IEEE Transactions on Circuits and Systems for Video Technology*, vol. 29, no. 8, pp. 2271–2284, 2019.
[32] G. Y. Gao and S. K. Tong and Z. H. Xia and B. Wu and L. Y. Xu and Z. Q. Zhao, "Reversible data hiding with automatic contrast enhancement for medical images," *Signal Processing*, vol. 178, 2021.
[33] H. T. Wu, J. W. Huang, and Y.-Q. Shi, "A reversible data hiding method with contrast enhancement for medical images," *Journal of Visual Communication and Image Representation*, vol. 31, pp. 146–153, 2015.
[34] R. C. Gonzalez and R. E. Woods, *Digital Image Processing (2nd Ed)*. Prentice Hall, New Jersey, USA, 1987.
[35] R. Gonzalez and R. Woods, "Digital image processing," in *Addison Wesley*, 1992.
[36] S. P. Jaiswal, O. C. Au, V. Jakhetiya, Y. F. Guo, A. K. Tiwari, and K. Yue, "Efficient adaptive prediction based reversible image watermarking," in *IEEE International Conference on Image Processing*, 2014, pp. 4540–4544.
[37] "USC-SIPI image database," *http://sipi.usc.edu/database*.
[38] Z. Jing, P. Han, Y. Li, and D. Peng, "Evaluation of focus measures in multi-focus image fusion," *Pattern Recognition Letters*, vol. 28, no. 4, pp. 493–500, 2007.
[39] X. Zhu and P. Milanfar, "Automatic parameter selection for denoising algorithms using a no-reference measure of image content," *IEEE Transactions on Image Processing*, vol. 19, no. 12, pp. 3112–3116, 2010.